# Mapping pressurized volcanic fluids from induced crustal seismic velocity drops

F. Brenguier *et al.*

*Science* **345**, 80 (2014);
DOI: 10.1126/science.1254073



*Science* (print ISSN 0036-8075; online ISSN 1095-9203) is published weekly, except the last week in December, by the American Association for the Advancement of Science, 1200 New York Avenue NW, Washington, DC 20005. 

Wind intensification in the California, Benguela, and Humboldt ecosystems could benefit marine populations by increasing nutrient input into subtropical euphotic zones if primary production is nutrient-limited. Large increases in wind strength, however, could be detrimental by disrupting trophic interactions (*18*), causing transport of planktonic organisms off continental shelves (*19*), or increasing acidic or hypoxic waters in shelf habitats (*4*, *5*). Although positive trends in coastal chlorophyll-a concentration off California and elsewhere (*20*) conform to the wind trends described here, there is no reason to assume that these changes will translate into increases in productivity across intermediate and higher trophic levels, although a recent study linked wind increases to improvements in albatross foraging efficiency and productivity (*21*). If new primary production constrains fisheries (*22*), greater primary productivity could enhance food production. However, ocean warming could counter stronger upwelling by increasing stratification (*23*), making it difficult to forecast ecological responses. Moreover, given the sensitivities of different species to the seasonality of upwelling (*24*, *25*), population variability might be linked to shifts in the phenology of upwelling as much as to changes in amplitude (*26*). Changes in the phenology of upwelling-favorable winds may also affect the trends within and across ecosystems described here. Ultimately, the sensitivity of observed wind trends to latitude, data type, season, and time-series duration demonstrated in this meta-analysis highlights the need for sustained high-quality observations of coastal winds and emphasizes the complexity of forecasting the consequences of wind intensification for ecosystems.

## REFERENCES AND NOTES


1. D. Pauly, V. Christensen, *Nature* **374**, 255–257 (1995).
2. B. A. Block *et al.*, *Nature* **475**, 86–90 (2011).
3. S. C. Doney *et al.*, *Ann. Rev. Mar. Sci.* **4**, 11–37 (2012).
4. N. Gruber *et al.*, *Science* **337**, 220–223 (2012).
5. F. Chan *et al.*, *Science* **319**, 920 (2008).
6. A. Bakun, *Science* **247**, 198–201 (1990).
7. S. Solomon, D. Qin, M. Manning, Z. Chen, M. Marquis, K. B. Averyt, M. Tignor, H. L. Miller, Eds., *Climate Change 2007: The Physical Science Basis. Contribution of Working Group I to the Fourth Assessment Report of the Intergovernmental Panel on Climate Change* (Cambridge Univ. Press, Cambridge, 2007).
8. A. Bakun, D. B. Field, A. Redondo-Rodriguez, S. J. Weeks, *Glob. Change Biol.* **16**, 1213–1228 (2010).
9. Materials and methods are available as supplementary materials on *Science* Online.
10. N. Narayan, A. Paul, S. Mulitza, M. Schulz, *Ocean Sci.* **6**, 815–823 (2010).
11. T. E. Cropper, E. Hanna, G. R. Bigg, *Deep Sea Res. Part I Oceanogr. Res. Pap.* **86**, 94–111 (2014).
12. E. D. Barton, D. B. Field, C. Roy, *Prog. Oceanogr.* **116**, 167–178 (2013).
13. B. R. Thomas, E. C. Kent, V. R. Swail, D. I. Berry, *Int. J. Climatol.* **28**, 747–763 (2008).
14. F. P. Chavez, J. Ryan, S. E. Lluch-Cota, M. Niquen C, *Science* **299**, 217–221 (2003).
15. S. Häkkinen, P. B. Rhines, D. L. Worthen, *Science* **334**, 655–659 (2011).
16. H. Baumann, O. Doherty, *PLOS ONE* **8**, e67596 (2013).
17. J. W. Hurrell, Y. Kushnir, G. Ottersen, M. Visbeck, *Geophys. Monogr. Ser.* **134**, 1–35 (2003).
18. P. Cury, C. Roy, *Can. J. Fish. Aquat. Sci.* **46**, 670–680 (1989).
19. L. W. Botsford, C. A. Lawrence, E. P. Dever, A. Hastings, J. Largier, *Deep Sea Res. Part II Top. Stud. Oceanogr.* **53**, 3116–3140 (2006).
20. M. Kahru, R. M. Kudela, M. Manzano-Sarabia, B. G. Mitchell, *Deep Sea Res. Part II Top. Stud. Oceanogr.* **77-80**, 89–98 (2012).
21. H. Weimerskirch, M. Louzao, S. de Grissac, K. Delord, *Science* **335**, 211–214 (2012).
22. J. H. Ryther, *Science* **166**, 72–76 (1969).
23. J. A. McGowan, D. R. Cayan, L. M. Dorman, *Science* **281**, 210–217 (1998).
24. B. A. Black *et al.*, *Glob. Change Biol.* **17**, 2536–2545 (2011).
25. I. D. Schroeder *et al.*, *Mar. Ecol. Prog. Ser.* **393**, 211–223 (2009).
26. M. A. Snyder, L. C. Sloan, N. S. Diffenbaugh, J. L. Bell, *Geophys. Res. Lett.* **30**, 1823 (2003).


## ACKNOWLEDGMENTS


Support for this study was provided by NSF award no. 1130125, NOAA's Environmental Research Division, and donors to the Farallon Institute. D.S. was supported by the Australian Research Council's Collaborative Research Network. The data reported in this paper are tabulated in the supplementary materials; electronic files of the tabulated data are available upon request from the senior author and at www.faralloninstitute.org.


## SUPPLEMENTARY MATERIALS

www.sciencemag.org/content/345/6192/77/suppl/DC1
Materials and Methods
Figs. S1 and S2
Tables S1 to S7
References (*27*–*31*)


31 January 2014; accepted 30 May 2014
10.1126/science.1251635


EARTHQUAKE DYNAMICS

# Mapping pressurized volcanic fluids from induced crustal seismic velocity drops


**F. Brenguier,[1]* M. Campillo,[1] T. Takeda,[2] Y. Aoki,[3] N. M. Shapiro,[4] X. Briand,[1] K. Emoto,[2] H. Miyake[3]**



**Volcanic eruptions are caused by the release of pressure that has accumulated due to hot volcanic fluids at depth. Here, we show that the extent of the regions affected by pressurized fluids can be imaged through the measurement of their response to transient stress perturbations. We used records of seismic noise from the Japanese Hi-net seismic network to measure the crustal seismic velocity changes below volcanic regions caused by the 2011 moment magnitude ($M_w$) 9.0 Tohoku-Oki earthquake. We interpret coseismic crustal seismic velocity reductions as related to the mechanical weakening of the pressurized crust by the dynamic stress associated with the seismic waves. We suggest, therefore, that mapping seismic velocity susceptibility to dynamic stress perturbations can be used for the imaging and characterization of volcanic systems.**


Large volcanic eruptions are preceded by long-term pressure buildup in volcano magmatic and hydrothermal systems. Therefore, knowledge of the extent and state of these pressurized volcanic fluids at depth will help in the better anticipation of future eruptions. In particular, seismic tomography is often used to delineate volcano-feeding systems at different scales (*1*, *2*). However, a major difficulty of traditional seismic imaging of volcanoes is that the geological contrasts of the host rock might dominate the final tomographic images, which are only partially sensitive to the content and state of volcanic fluids (*3*).

Recent geodetic observations have shown that volcanic areas are characterized by anomalous responses to crustal deformation induced by large earthquakes, as demonstrated by the subsidence of volcanoes in Chile and Japan after the 2010 Maule and 2011 Tohoku-Oki earthquakes (*4*, *5*). This sensitivity to strong coseismic deformation and shaking is probably associated with the presence of pressurized hydrothermal and magmatic fluids at depth in a fractured medium. We explored the responses of volcanoes to transient stress perturbations by investigating the temporal evolution of crustal seismic velocities in Japan in response to the seismic shaking and deformation caused by the March 2011 moment magnitude ($M_w$) 9.0 Tohoku-Oki earthquake.

The Hi-net, Japanese high-sensitivity seismograph network, is among the densest in the world; thus, the 2011 Tohoku-Oki earthquake remains the best-recorded large earthquake to date. It was associated with large, widespread static ground deformation and ground shaking (Fig. 1). In this study, we used seismic noise-based monitoring (*6*) to characterize the response of the upper crust to the coseismic shaking and deformation caused by the earthquake. We analyzed 1 year of continuous seismic records from a portion of the dense Hi-net seismic network (600 stations, as shown in the inset to Fig. 1A), spanning from 6 months before to 6 months after the earthquake occurrence.

We computed the daily vertical-vertical noise cross-correlation functions using a processing scheme that minimized the effects of the strong aftershock activity that followed the Tohoku-Oki


[1]Institut des Sciences de la Terre, Université Joseph Fourier, CNRS, F-38041 Grenoble, France. [2]National Research Institute for Earth Science and Disaster Prevention, Tsukuba, Japan. [3]Earthquake Research Institute, University of Tokyo, Tokyo, Japan. [4]Institut de Physique du Globe de Paris, Sorbonne Paris Cité, CNRS (UMR7154), 75238 Paris Cedex 5, France.
*Corresponding author. E-mail: florent.brenguier@ujf-grenoble.fr

earthquake (*7*). To avoid the choice of an arbitrary reference cross-correlation function and to improve the precision of the measurements, we separately computed velocity changes for all of the possible daily cross-correlation functions for each station pair. Using a Bayesian least-squares inversion, we retrieved accurate daily continuous velocity change time series for every station pair (*7*).

We computed the seismic velocity changes averaged over the day of the Tohoku-Oki earthquake and 4 days after, relative to the seismic velocity changes time series averaged over 6 months before the Tohoku-Oki earthquake (Fig. 2A) (*7*). These changes mainly correspond to the response of the upper crust to the coseismic shaking and deformation. Similar to previous studies of coseismic velocity variations (*6*, *8*), a reduction in velocity was widespread over Honshu Island. Furthermore, the strongest velocity drops were not observed in the area closest to the epicenter or within large sedimentary basins, as would be expected. The patterns of the observed velocity reductions did not correlate with the intensity of the ground shaking or with the coseismic deformation (Fig. 1); instead, the strongest coseismic velocity reductions occurred under volcanic regions. In particular, a large part of the Tohoku volcanic front and the Mt. Fuji volcanic region are well delineated.

The mechanism by which seismic velocities decrease in response to stress perturbations is commonly described as related to the opening of cracks (*9*, *10*), which might also induce an increase in permeability and a transfer of fluids at depth and may lead to further triggering of earthquakes. Over long distances, large earthquakes

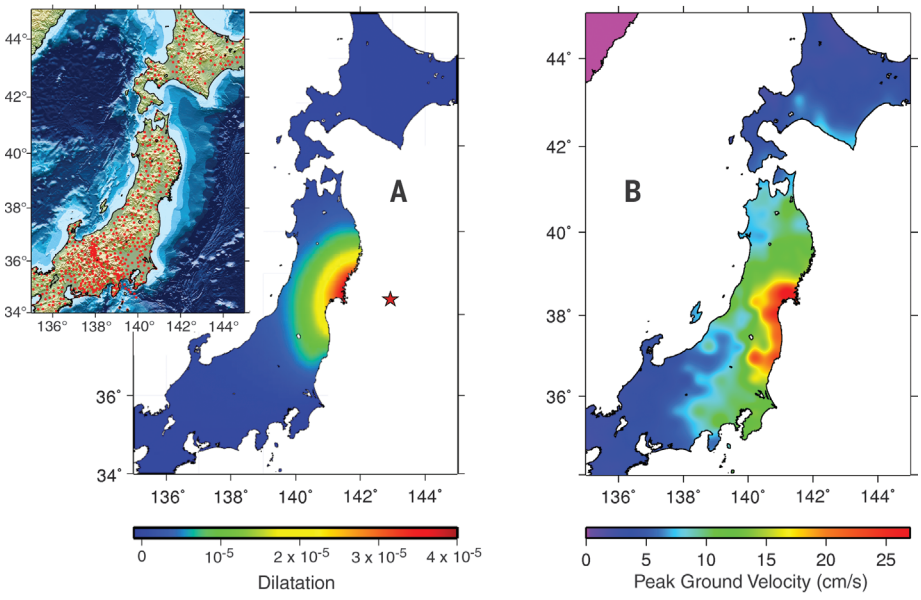


**Fig. 1. Static strain and ground shaking caused by the Tohoku-Oki earthquake.** (**A**) Modeled coseismic dilatation static strain at 5 km in depth (*7*). The red star shows the position of the epicenter of the Tohoku-Oki earthquake. (Inset) Positions of the Hi-net seismic stations (red points). (**B**) Averaged peak ground velocity measured using the KiK-net strong-motion network (*7*).

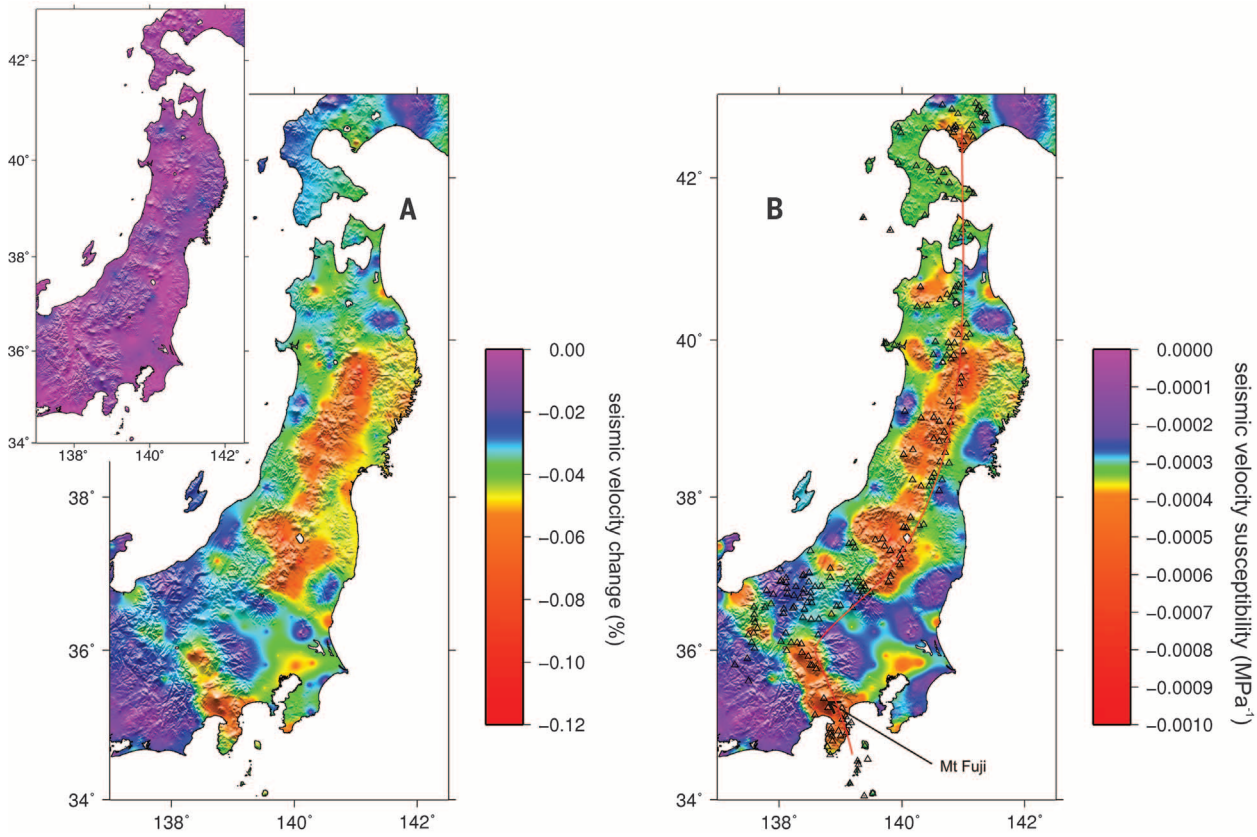


**Fig. 2. Crustal seismic velocity perturbations caused by the Tohoku-Oki earthquake.** (**A**) Coseismic crustal seismic velocity changes induced by the 2011 Tohoku-Oki earthquake. (Inset) Velocity changes averaged over 5 days preceding the day of the Tohoku-Oki earthquake. (**B**) Seismic velocity susceptibility computed using the seismic velocity changes shown in (A). Black triangles denote Quaternary period volcanoes, and the red line depicts the main volcanic fronts.

are known to trigger anomalous hydrothermal activity (*11*), aftershocks on a global scale (*12*), tectonic tremor activity (*13*), and slow-slip events (*14*). The origin for this remote triggering of activity is believed to be the associated dynamic stress that is caused by the passing of the seismic waves.

We used the approach of Gomberg and Agnew (*15*) to estimate the level of dynamic strain $\Delta\xi$ and dynamic stress $\Delta\sigma$ from the observed peak ground velocity (PGV), such that $\Delta\xi \approx v/c$ and $\Delta\sigma \approx \mu v/c$, where $\mu$ is the mean crustal shear modulus ($\sim 30 \times 10^9$ Pa), $v$ is the PGV (measured by the KiK-net, strong-motion seismograph network installed in boreholes together with the Hi-net sensors), and $c$ is the mean wave phase velocity of the Rayleigh waves that propagate within the upper crust (~3 km/s). The dynamic strain caused by the passing of the seismic waves was one to two orders of magnitude higher than the static coseismic strain for Honshu Island. We thus conclude that the dynamic stress associated with the seismic waves emitted by the Tohoku-Oki earthquake was the main cause of the large seismic velocity reductions under the volcanic regions—in particular, the Mt. Fuji area, where the static stress change can be considered negligible. We then defined the seismic velocity susceptibility as the ratio between the observed reductions in the seismic velocity and the estimated dynamic stress. The distribution of these seismic velocity susceptibilities correlates with the main volcanic areas (Fig. 2B).

The sensitivity of the seismic velocity to stress changes in the rock increases with decreasing effective pressure (*16*, *17*). Under volcanic areas, the effective pressure in the crust can be reduced because of the presence of highly pressurized hydrothermal and magmatic volcanic fluids at depth. We thus argue that the observed strong coseismic velocity reductions delineate the regions where such pressurized volcanic fluids are present in the upper crust. An important implication of our observation is that the seismic velocity susceptibility to stress can be used as a proxy to the level of pressurization of the hydrothermal and/or magmatic fluids in volcanic areas. So far, this susceptibility is greatest in the Mt. Fuji area and along the Tohoku volcanic arc, where it reached $15 \times 10^{-4}$ MPa$^{-1}$, whereas it is more than 10 times smaller for the Cretaceous stiff plutonic regions of eastern Tohoku (Fig. 2B).

Fluids are also known to have important roles in earthquake nucleation (*3*). The volcanic areas where large seismic velocity susceptibility was observed were also characterized by large triggered seismic activity after the Tohoku-Oki earthquake (*18*, *19*), including a particularly strong (magnitude 6.4) earthquake that occurred 4 days after the main shock, near Mt. Fuji. This confirms that the crust in these areas is quite sensitive to strong transient stress perturbations. We argue that mapping the susceptibility of seismic velocities to dynamic stress changes can be used to image and characterize regions with low effective pressure, such as volcanic systems.


## REFERENCES AND NOTES

1. S. Husen, R. B. Smith, G. P. Waite, *J. Volcanol. Geotherm. Res.* **131**, 397–410 (2004).
2. J. M. Lees, *J. Volcanol. Geotherm. Res.* **167**, 37–56 (2007).
3. D. Zhao, O. P. Mishra, R. Sanda, *Phys. Earth Planet. Inter.* **132**, 249–267 (2002).
4. M. E. Pritchard, J. A. Jay, F. Aron, S. T. Henderson, L. E. Lara, *Nat. Geosci.* **6**, 632–636 (2013).
5. Y. Takada, Y. Fukushima, *Nat. Geosci.* **6**, 637–641 (2013).
6. F. Brenguier *et al.*, *Science* **321**, 1478–1481 (2008).
7. See supplementary materials on *Science* Online.
8. U. Wegler, C. Sens-Schönfelder, *Geophys. J. Int.* **168**, 1029–1033 (2007).
9. L. H. Adams, E. D. Williamson, *J. Franklin Inst.* **195**, 475–529 (1923).
10. D. A. Lockner, J. B. Walsh, J. D. Byerlee, *J. Geophys. Res.* **82**, 5374–5378 (1977).
11. S. Husen, R. Taylor, R. B. Smith, H. Healser, *Geology* **32**, 537–540 (2004).
12. F. F. Pollitz, R. S. Stein, V. Sevilgen, R. Bürgmann, *Nature* **490**, 250–253 (2012).
13. J. L. Rubinstein *et al.*, *Nature* **448**, 579–582 (2007).
14. D. Zigone *et al.*, *J. Geophys. Res.* **117**, B09304 (2012).
15. J. Gomberg, D. Agnew, *Bull. Seismol. Soc. Am.* **86**, 212–220 (1996).
16. B. Zinszner, P. A. Johnson, P. N. J. Rasolofosaon, *J. Geophys. Res.* **102**, 8105–8120 (1997).
17. S. A. Shapiro, *Geophysics* **68**, 482–486 (2003).
18. F. Hirose, K. Miyaoka, N. Hayashimoto, T. Yamazaki, M. Nakamura, *Earth Planets Space* **63**, 513–518 (2011).
19. Y. Yukutake *et al.*, *Earth Planets Space* **63**, 737–740 (2011).



## ACKNOWLEDGMENTS

All of the seismological data used in this study are archived at the Japanese National Research Institute for Earth Science and Disaster Prevention (NIED) (www.hinet.bosai.go.jp/?LANG=en and www.kyoshin.bosai.go.jp/). The seismological data used in this study are available upon request at the NIED data center. We thank Geospatial Information Authority of Japan for access to Global Navigation Satellite System data. All of the computations in this study were performed using the High-Performance Computing (CIMENT) infrastructure (https://ciment.ujf-grenoble.fr), which is supported by the Rhône-Alpes region (GRANT CPER07_13 CIRA: www.ci-ra.org), France Grilles (www.france-grilles.fr), and the CNRS MASTODONS program. We acknowledge the French National Research Agency and the Japan Science and Technology Agency for funding support (project 2011-JAPN-006-NAMAZU). We received support from the European Union through the projects European Research Council advanced grant 227507 "Whisper" and FP7 RI283542 "VERCE." We thank T. Nishimura, P. Johnson, G. Olivier, G. Hillers, C. Jaupart, and T. Lecocq for useful discussions.


## SUPPLEMENTARY MATERIALS

www.sciencemag.org/content/345/6192/80/suppl/DC1
Materials and Methods
Figs. S1 and S2
References (*20*–*32*)

28 March 2014; accepted 19 May 2014
10.1126/science.1254073

NEURODEVELOPMENT

# Parasympathetic neurons originate from nerve-associated peripheral glial progenitors

**Vyacheslav Dyachuk,[1,2]* Alessandro Furlan,[1]* Maryam Khatibi Shahidi,[3] Marcela Giovenco,[1] Nina Kaukua,[4] Chrysoula Konstantinidou,[5] Vassilis Pachnis,[5] Fatima Memic,[1] Ulrika Marklund,[1] Thomas Müller,[6] Carmen Birchmeier,[6] Kaj Fried,[4] Patrik Ernfors,[1]†‡ Igor Adameyko[7]†‡**

**The peripheral autonomic nervous system reaches far throughout the body and includes neurons of diverse functions, such as sympathetic and parasympathetic. We show that the parasympathetic system in mice—including trunk ganglia and the cranial ciliary, pterygopalatine, lingual, submandibular, and otic ganglia—arise from glial cells in nerves, not neural crest cells. The parasympathetic fate is induced in nerve-associated Schwann cell precursors at distal peripheral sites. We used multicolor Cre-reporter lineage tracing to show that most of these neurons arise from bi-potent progenitors that generate both glia and neurons. This nerve origin places cellular elements for generating parasympathetic neurons in diverse tissues and organs, which may enable wiring of the developing parasympathetic nervous system.**

Almost all bodily functions are regulated by the autonomic nervous system. Most autonomic neurons arise from migrating neural crest cells, at least in the chick (*1*, *2*). However, unlike the neural crest–derived sympathetic, sensory, and enteric nervous systems, for which the migratory paths and cellular origins have been studied in detail, little is known about the developmental origin of the parasympathetic nervous system. Available data have been difficult to reconcile in the mouse because migration of the cranial neural crest ceases around embryonic day 10 (E10), although cranial parasympathetic ganglia do not coalesce until around E12 (*3*, *4*). Schwann cell precursors associated with nerves produce myelinating and nonmyelinating Schwann cells, endoneural fibroblasts, and melanocytes during development (*5*) and can therefore be considered as multipotent stem-like cells. The role of Schwann cell precursors

[1]Unit of Molecular Neurobiology, Department of Medical Biochemistry and Biophysics, Karolinska Institutet, Stockholm, Sweden. [2]A.V. Zhirmunsky Institute of Marine Biology of the Far Eastern Branch of the Russian Academy of Sciences, Vladivostok, Russia. [3]Department of Dental Medicine, Karolinska Institutet, Stockholm, Sweden. [4]Department of Neuroscience, Karolinska Institutet, Stockholm, Sweden. [5]Division of Molecular Neurobiology, Medical Research Council (MRC) National Institute for Medical Research, London, UK. [6]Department of Neuroscience, The Max Delbrück Center for Molecular Medicine, Berlin-Buch, Germany. [7]Department of Physiology and Pharmacology, Karolinska Institutet, Stockholm, Sweden. *These authors contributed equally to this work. †These authors contributed equally to this work. **‡Corresponding author. E-mail: igor.adameyko@ki.se (I.A.); patrik.ernfors@ki.se (P.E.)**